scientific **data**

Check for updates

OPEN

DATA DESCRIPTOR

Single-cell transcriptome dataset of human and mouse in vitro adipogenesis models

Jiehan Li[1,2,3,8], Christopher Jin[1,8], Stefan Gustafsson[4], Abhiram Rao[5], Martin Wabitsch [6], Chong Y. Park[1,2,3], Thomas Quertermous[1,3], Joshua W. Knowles[1,2,3,7 ✉] & Ewa Bielczyk-Maczynska[1,2,3 ✉]

Adipogenesis is a process in which fat-specific progenitor cells (preadipocytes) differentiate into adipocytes that carry out the key metabolic functions of the adipose tissue, including glucose uptake, energy storage, and adipokine secretion. Several cell lines are routinely used to study the molecular regulation of adipogenesis, in particular the immortalized mouse 3T3-L1 line and the primary human Simpson-Golabi-Behmel syndrome (SGBS) line. However, the cell-to-cell variability of transcriptional changes prior to and during adipogenesis in these models is not well understood. Here, we present a single-cell RNA-Sequencing (scRNA-Seq) dataset collected before and during adipogenic differentiation of 3T3-L1 and SGBS cells. To minimize the effects of experimental variation, we mixed 3T3-L1 and SGBS cells and used computational analysis to demultiplex transcriptomes of mouse and human cells. In both models, adipogenesis results in the appearance of three cell clusters, corresponding to preadipocytes, early and mature adipocytes. These data provide a groundwork for comparative studies on these widely used *in vitro* models of human and mouse adipogenesis, and on cell-to-cell variability during this process.

Background & Summary

Adipose tissue carries out multiple roles that affect whole-body metabolism. In addition to storing energy in the form of lipids, it contributes to the homeostatic maintenance of blood glucose levels by taking up glucose in response to insulin and regulates the function of other metabolic organs by secreting hormones such as leptin and adiponectin[1,2].

Adipogenesis is a differentiation process in which fat-specific progenitor cells (preadipocytes) convert into adipocytes, which carry out key metabolic functions of the adipose tissue. *In vivo*, preadipocytes are located in proximity of blood vessels within adipose tissue and contribute to adipose tissue maintenance and expansion in obesity[3]. Dysregulation of adipogenesis can result in metabolic disease, including insulin resistance and type 2 diabetes[4].

Several preadipocyte *in vitro* models are routinely used to study the molecular regulation of adipogenesis. The most commonly used *in vitro* models include the immortalized mouse 3T3-L1 cell line[5] and the primary, non-immortalized, non-transformed human Simpson-Golabi Behmel syndrome (SGBS) cell line[6]. These cellular models brought on major breakthroughs in our understanding of molecular mechanisms of adipogenic differentiation, both in development and in obesity[7,8]. However, adipogenic models show high levels of cell-to-cell heterogeneity in their differentiation responses to stimuli[9]. This heterogeneity can be due to multiple factors, including variations in preadipocyte commitment and stochasticity of responses to differentiation

[1]Division of Cardiovascular Medicine, Department of Medicine, Stanford University School of Medicine, Stanford, CA, 94305, USA. [2]Stanford Diabetes Research Center, Stanford University School of Medicine, Stanford, CA, 94305, USA. [3]Stanford Cardiovascular Institute, Stanford University School of Medicine, Stanford, CA, 94305, USA. [4]Clinical Epidemiology Unit, Department of Medical Sciences, Uppsala University, Uppsala, Sweden. [5]Department of Bioengineering, Stanford University, Stanford, CA, 94305, USA. [6]Department of Pediatrics and Adolescent Medicine, Center for Rare Endocrine Diseases, Division of Pediatric Endocrinology and Diabetes, Ulm University Medical Centre, Ulm, 89075, Germany. [7]Stanford Prevention Research Center, Stanford University School of Medicine, Stanford, CA, 94305, USA. [8]These authors contributed equally: Jiehan Li, Christopher Jin. ✉e-mail: knowlej@stanford.edu; ewabm@stanford.edu
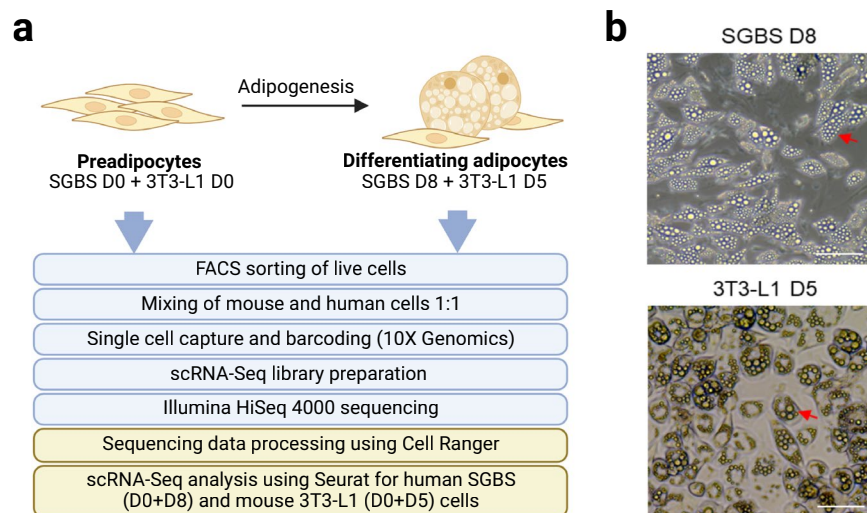
Fig. 1 scRNA-Seq of mouse and human adipogenesis. (**a**) Schematic of the workflow. Human SGBS and mouse 3T3-L1 cells were analyzed at two time points, corresponding to before (D0) and during (D5 for 3T3-L1, D8 for SGBS) adipogenesis. At each time point, live cells were purified using exclusion of propidium iodide-stained cells by FACS. Equal numbers of SGBS and 3T3-L1 cells were then mixed and subjected to microfluidic single-cell capture with GelBeads-in-emulsion (GEMs) using 10X Chromium Controller. Single-cell cDNA libraries were prepared using the Chromium Single Cell 3′ Library & Gel Bead Kit (10X Genomics), followed by sequencing on Illumina HiSeq 4000. Computational analysis involved barcode processing, UMI counting, demultiplexing, gene and cell filtering, normalization, and clustering. (**b**) Representative light microscopy images of differentiated cells, SGBS at day 8 (D8) and 3T3-L1 at day 5 (D5), show similar pattern of lipid deposition in adipocytes (arrows). Scale bar: 50 μm.

stimuli. Despite that, adipogenesis is often studied using bulk approaches, such as bulk RNA-Sequencing, which ignore the variability between individual cells, likely masking the presence of distinct cell subpopulations during adipogenesis.

Here, we present a single-cell RNA-Sequencing (scRNA-Seq) dataset collected before and during adipogenic differentiation of 3T3-L1 and SGBS cells to allow for analyses of heterogeneity of transcriptional states before and during adipogenesis, as well as comparisons between mouse and human models of adipogenesis. To minimize technical variation, at two time points (before and during adipogenic differentiation) mouse and human cells were mixed in equal ratios and subjected to scRNA-Seq, followed by computational demultiplexing and separation of data from mouse and human cells (Fig. 1a). The time points were selected based on previously established time course comparison of adipogenesis in SGBS and 3T3-L1 cells[10] and validated using light microscopy (Fig. 1b). Analysis of cells at later timepoints was not feasible due to the fragility of large adipocytes, which would preclude single-cell analysis. Through technical validation, we demonstrate quality of this dataset. By unsupervised clustering we identify cell populations that correspond to preadipocytes, differentiating and mature adipocytes in both models.

This dataset complements recent advances in characterizing the transcriptome of adipose tissue in human and mice at a single-cell[11–14] and single-nucleus level[15], which revealed significant level of transcriptional heterogeneity within both adipose progenitor cells and adipocytes. In addition, the progress in adipocyte cell culture led to establishment of new models with improved translational relevance over cell lines. For example, our dataset can be used as a point of reference for the investigation using other models of adipogenesis, including primary adipocyte precursor cells (APCs)[16,17] and adipose mesenchymal stem cells (AMSCs)[18,19]. In addition, transcriptome data from differentiated SGBS and 3T3-L1 cells can be utilized to compare with *in vitro* adipocyte biology models, such as cultured primary adipocytes[20].

Methods

Cell culture. The 3T3-L1 preadipocyte cell line was maintained in Dulbecco's Modified Eagle's Medium (DMEM, Thermo Fisher) with 10% Fetal Bovine Serum (GeminiBio, lot #A22G00J), 100 units/ml penicillin and 100 μg/ml streptomycin, in a humidified 5% CO2 incubator. Cells were used at passage 7. For adipogenic differentiation cells were grown to confluency. 48 h past confluency, some of the cells were collected for scRNA-Seq analysis before adipogenesis (day 0, D0), while other cells were differentiated by stimulation with 1 μM dexamethasone, 0.5 mM IBMX, 10 μg/ml insulin in growth medium. After 48 h the medium was changed to growth medium with 10 μg/ml insulin in growth medium until day 5 (D5), when the cells were collected for scRNA-Seq analysis during adipogenesis.

The SGBS cell line was cultured and differentiated as previously described[6], and used at passage 34. Cells were maintained in a humidified chamber at 37 °C with 5% CO_2, and the media was replaced every 2-3 days. The standard culture media used was composed of DMEM/Nutrient Mix F-12 (Invitrogen), supplemented with
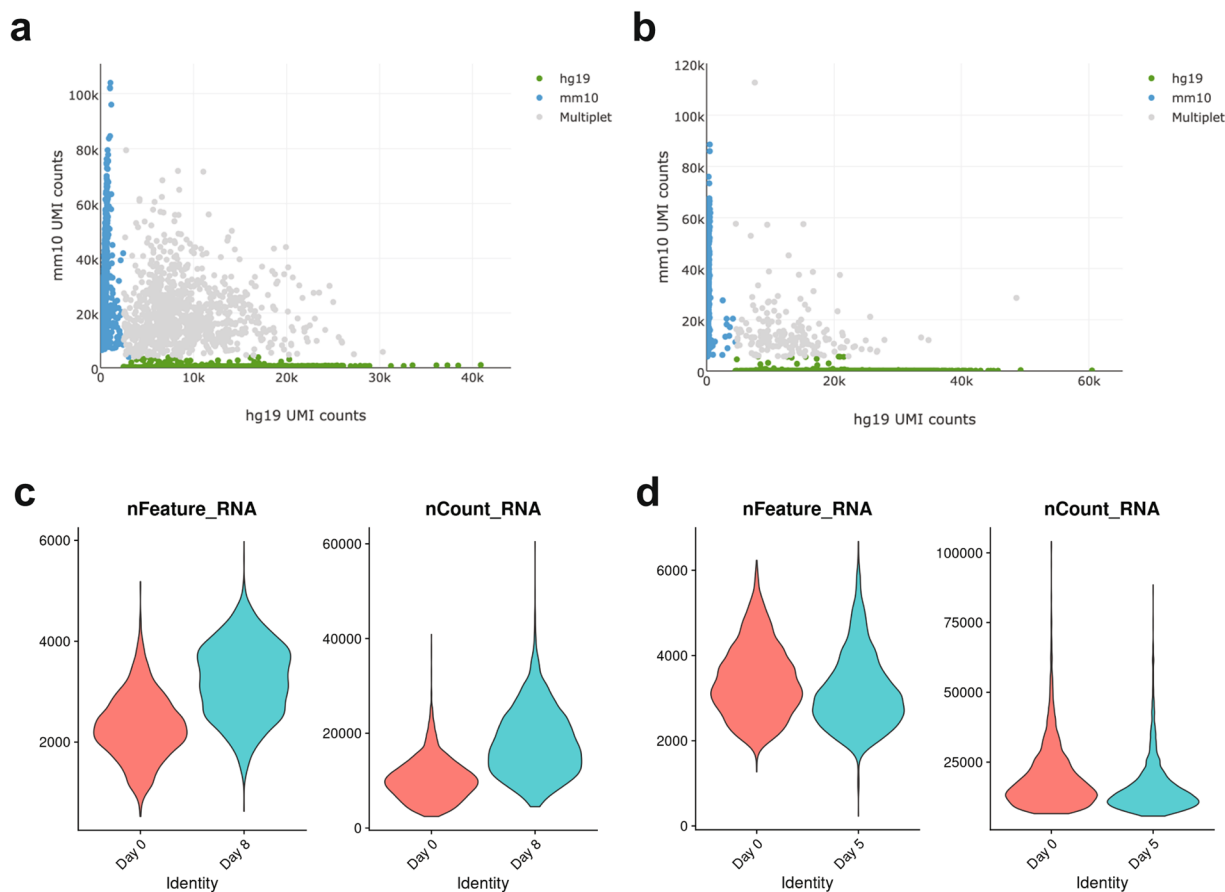
Fig. 2 Single-cell RNA-Seq dataset quality assessment following inferring the species from transcriptome. (**a,b**) Plots representing quantification of the alignment of individual cell's transcriptomes to the human (hg19) and mouse (mm10) genomes at (**a**) D0 3T3-L1/D0 SGBS, and (**b**) D5 3T3-L1/D8 SGBS. (**c,d**) Violin plots of gene counts (nFeature_RNA) and UMI counts (nCount_RNA) after quality control filtering in (**c**) SGBS cells and (**d**) 3T3-L1 cells, separated by the day of differentiation.

Raw sequencing sample	SGBS D0, 3T3-L1 D0		SGBS D8, 3T3-L1 D5	
Number of reads	320,829,287		334,091,518	
Q30 bases in barcodes	96.9%		97.5%	
Q30 bases in RNA reads	76.7%		77.4%	
Q30 bases in UMI reads	96.8%		97.6%	
Mean reads per cell	31,460		49,239	
Processed sample	**SGBS D0**	**3T3-L1 D0**	**SGBS D8**	**3T3-L1 D5**
Reads mapped to genome	30.8%	58.1%	51.1%	41.7%
Reads mapped to exons	25.6%	46.8%	43.2%	33.7%
Reads mapped uniquely to genome	29.8%	52.6%	49.8%	38.5%
Estimated number of cells	5,672	5,402	3,655	3,305
Fraction of reads in cells	94.40%	94.50%	93.2%	93.3%
Median genes per cell	2,239	3,360	3,199	3,011
Total genes detected	19,339	17,013	19,862	16,444

Table 1. Detailed QC report of 10X Genomics sequencing files (Cell Ranger).

33 uM biotin, 17 uM pantothenic acid, 10% FBS and antibiotics (100 IU/ml penicillin and 100 ug/ml strep-tomycin). Cells were cultured for three days post-confluence, and either subjected to scRNA-Seq (D0, before differentiation) or differentiated. Differentiation was induced by the change of culture media to DMEM/F-12, 33 uM biotin, 17 uM pantothenic acid, 0.01 mg/ml human transferrin, 100 nM cortisol, 200 pM triiodothyro-nine, 20 nM human insulin (Sigma-Aldrich), 25 nM dexamethasone, 250 uM IBMX, 2 uM rosiglitazone, and antibiotics. After four days of differentiation, the medium was replaced with DMEM/F-12, 33 uM biotin, 17 uM

	SGBS D0	SGBS D8	3T3-L1 D0	3T3-L1 D5
Unfiltered cells	5,672	3,655	5,402	3,305
Filtered cells	4,742	3,480	4,526	3,118
Filtered genes detected	16,486	17,178	14,755	14,436

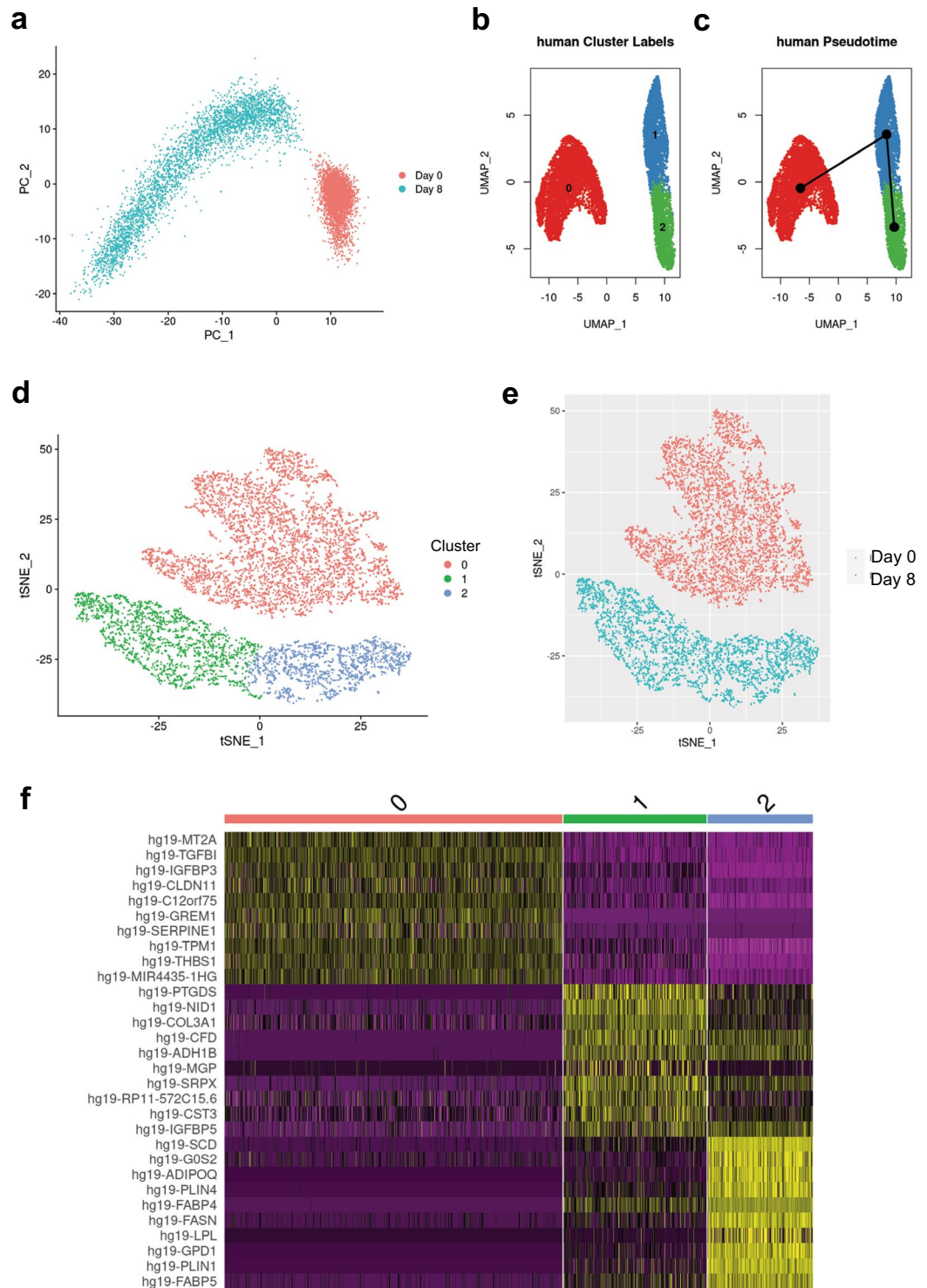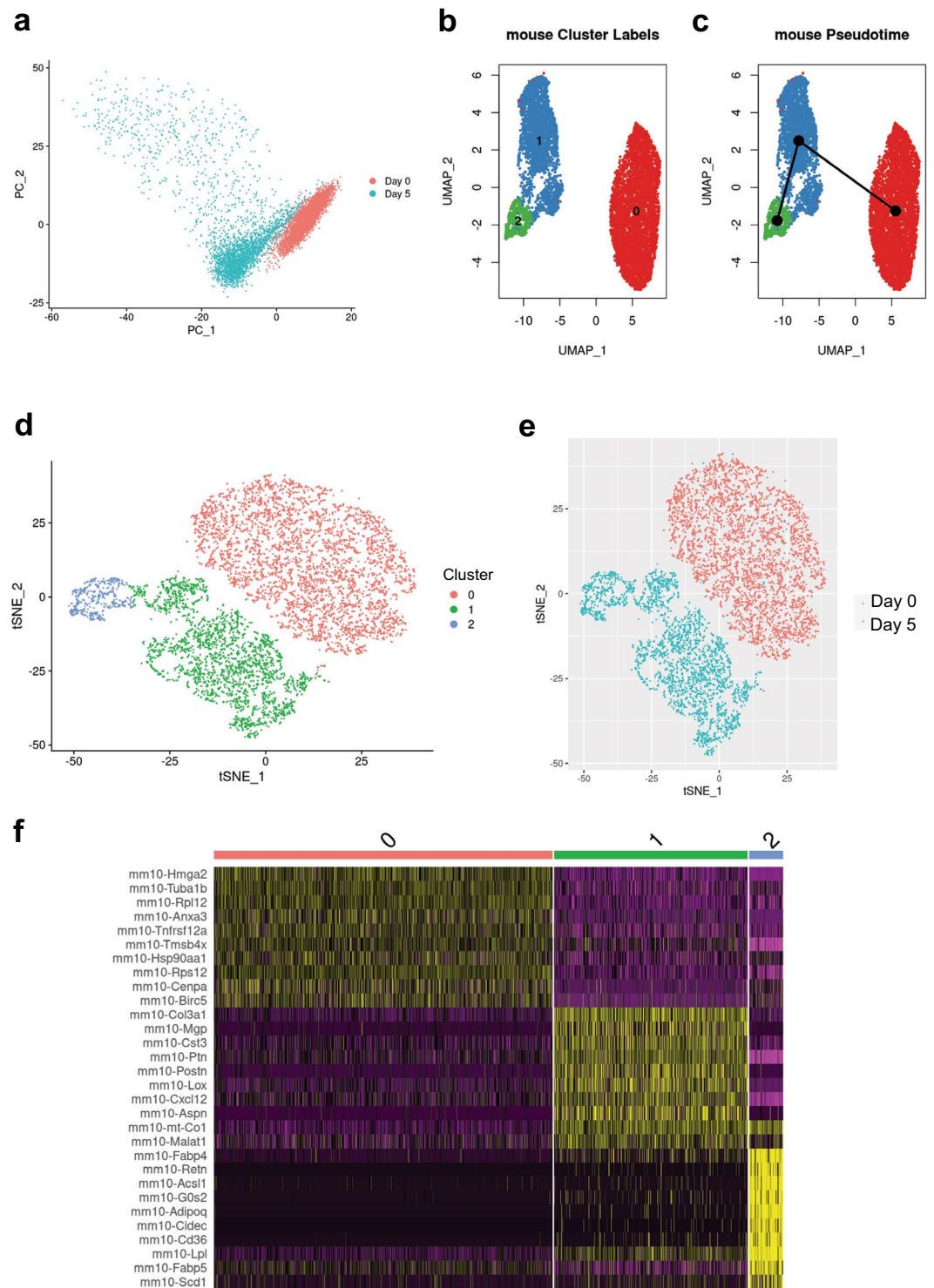**Table 2.** Final cell quantification statistics.

Fig. 3 Clustering of scRNA-Seq data in human SGBS cells. (**a**) Primary component analysis (PCA) plot. (**b**) UMAP plot. (**c**) Pseudotime analysis. (**d**) t-SNE plot. (**e**) Assignment of cells by differentiation day (D0 vs. D8), superimposed on the t-SNE plot. (**f**) Heatmap showing the expression of top 10 enriched genes per cell cluster.

Fig. 4 Clustering of scRNA-Seq data in murine 3T3-L1 cells. (**a**) Primary component analysis (PCA) plot. (**b**) UMAP plot. (**c**) Pseudotime analysis. (**d**) t-SNE plot. (**e**) Assignment of cells by differentiation day (D0 vs. D5), superimposed on the t-SNE plot. (**f**) Heatmap showing the expression of top 10 enriched genes per cell cluster.

pantothenic acid, 0.01 mg/ml human transferrin, 100 nM cortisol, 200 pM triiodothyronine, 20 nM human insulin and antibiotics. SGBS cells were cultured for eight days after the induction of differentiation and subjected to scRNA-Seq analysis (time point during differentiation, D8).

Both cell types were cultured in 6-well polystyrene tissue culture plates (Falcon, #353046).

Microscopy. Cultured cells were imaged using EVOS XL Core (Thermo Fisher Scientific) at 20X magnification.
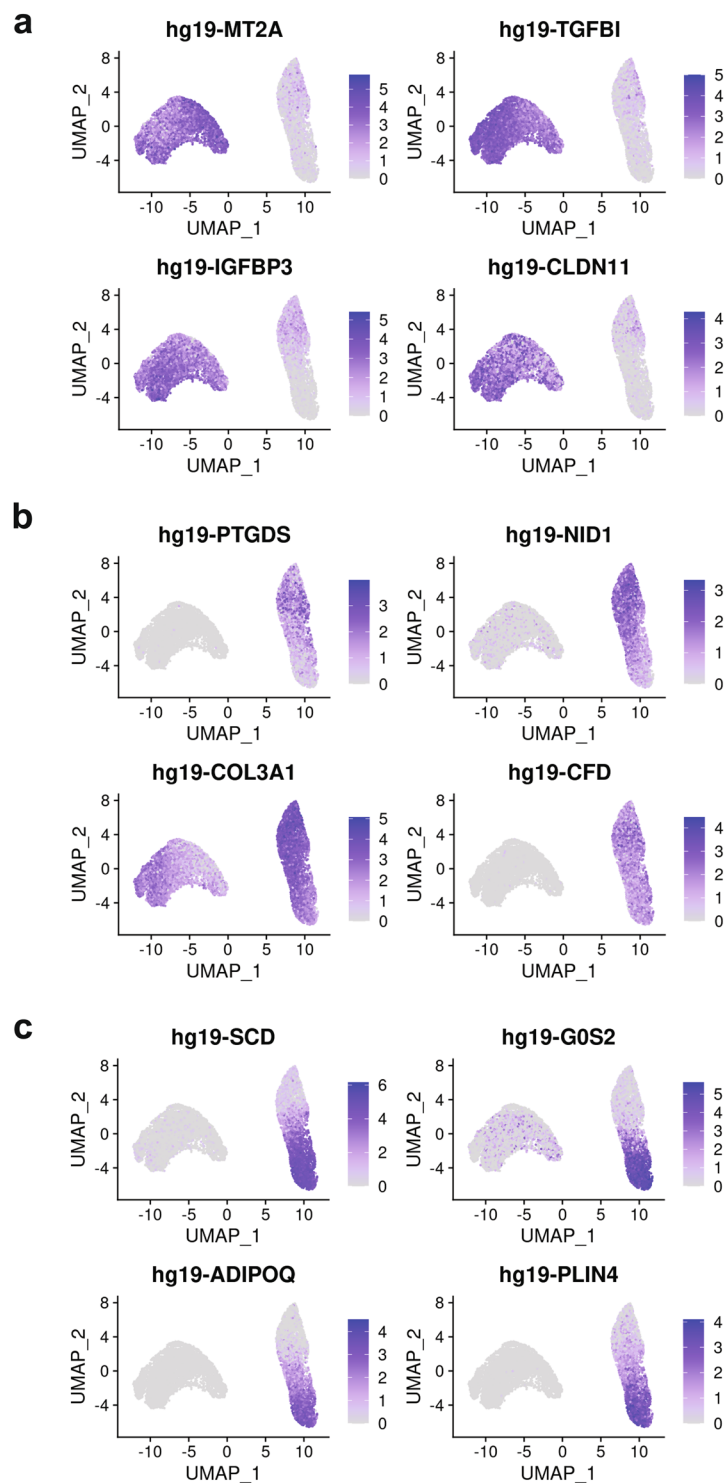
Fig. 5 Feature plots showing the expression of cluster marker genes for individual clusters in human SGBS cells. (**a**) Cluster 0 (preadipocytes); (**b**) Cluster 1 (differentiating); (**c**) Cluster 2 (adipocytes).

Single-cell sorting and cDNA library preparation.   On the day of collection, cells were detached from culture plates using TrypLE Select Enzyme (Gibco), centrifuged at $300 \times$ g for 5 min and resuspended in PBS with 0.04% Bovine Serum Albumin. Lack of staining with Trypan Blue Solution (Gibco) was used to sort live cells using Influx sorter (Beckman Dickinson), with >95% of single cells quantified as live in all experiments. Equal numbers of sorted live SGBS and 3T3-L1 cells were mixed and subjected to single-cell capture on the 10X Chromium Controller device at Stanford Genomics Service Center during which single cells were encapsulated with individual Gel Beads-in-emulsion (GEMs) using the Chromium Single Cell 3′ Library & Gel Bead Kit (10X Genomics). The number of cells targeted in each experiment was 10,000, following manufacturer's guidelines.
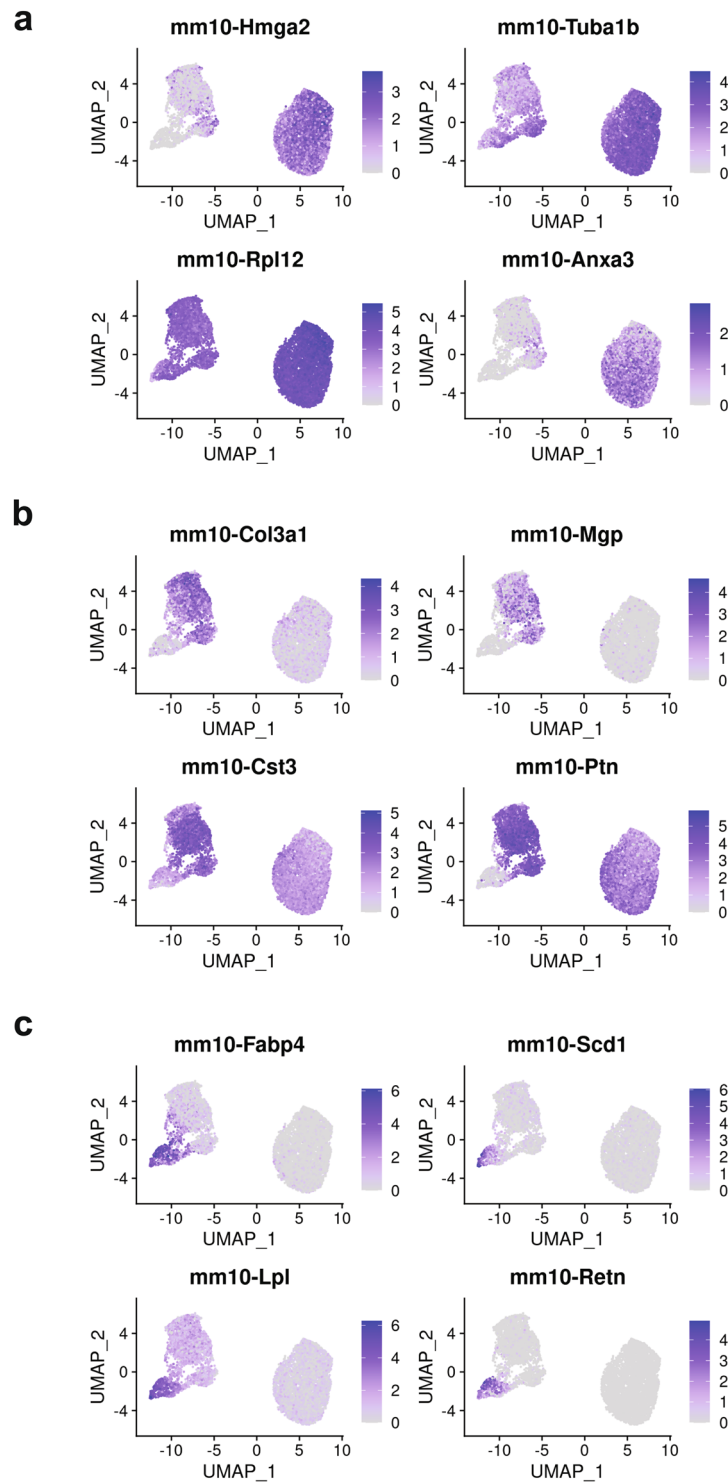
Fig. 6 Feature plots showing the expression of cluster marker genes for individual clusters in mouse 3T3-L1 cells. (**a**) Cluster 0 (preadipocytes); (**b**) Cluster 1 (differentiating); (**c**) Cluster 2 (adipocytes).

In-drop reverse transcription and cDNA amplification was conducted according to the manufacturer's protocol to construct expression libraries. Library size was checked using Agilent Bioanalyzer 2100 at the Stanford Genomics facility. The libraries were sequenced using Illumina HiSeq 4000.

Raw data processing.   Cell Ranger v2.10 was used for processing and analysing the raw single cell FASTQ files. The following genome builds were used: mm10 for the mouse genome, hg19 for the human genome. Quality control (QC) steps that were taken to assess the quality of the sequencing data and to identify potential included: sample demultiplexing, read alignment and filtering, gene expression quantification, cell filtering and QC metrics,
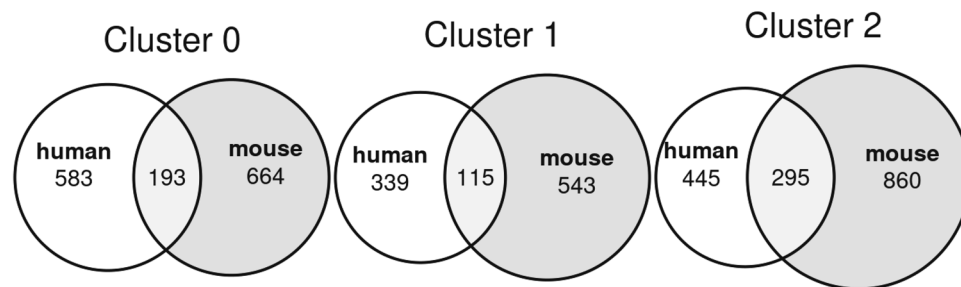
Fig. 7 Venn diagram representation of the number of unique and shared marker genes between SGBS and 3T3-L1 cell lines, separated by cell cluster.

Cell line	Cluster number and description	Top 5 enriched genes	Number of cells	% All cells
SGBS	0 – preadipocytes	*MT2A, TGFBI, IGFBP3[31], CLDN11[23], C12orf75*	4,744	57.70
	1 – differentiating	*PTGDS[32], NID1[33], COL3A1[24], CFD[34], ADH1B[35]*	2,002	24.35
	2 – adipocytes	*SCD[36], G0S2[37], ADIPOQ[27], PLIN4[28], FABP4[25,26]*	1,476	17.95
3T3-L1	0 – preadipocytes	*Hmga2[38], Tuba1b, Rpl12, Anxa3[39], Tnfrsf12a[40]*	4,574	59.84
	1 – differentiating	*Col3a1[24], Mgp[41], Cst3, Ptn, Postn*	2,612	34.17
	2 – adipocytes	*Fabp4[25,26], Scd1[36], Lpl[29], Retn[30], Acsl1[42]*	458	5.99

Table 3. Description of cell clusters identified by unsupervised clustering.

and data normalization and batch correction. The batch correction was performed with the Seurat base function "MergeSeurat". 10,198 cells passed the QC when D0 SGBS and D0 3T3-L1 cells were analysed, compared to 6,785 cells when D5 3T3-L1 and D8 SGBS cells were analysed. Only reads mapping to mm10 or hg19 were used for downstream processing. Genome mapping was used to assign each cell as either human or mouse.

Bioinformatic analysis of scRNA-Seq data. Seurat v4.3[21] was used to merge processed data for two single-cell sequencing runs, combining sequencing data from different stages of adipocyte differentiation. The data was first split between human and mouse data, pre-processed using Seurat, then log normalized. The major variable features within the processed data were identified using Variance Stabilizing Transformation. The gene matrix was then visualized and analysed using principal component analysis (PCA), with gene associations to each principal component displayed. Seurat's *FindNeighbors* and *FindClusters* functions (resolution = 0.09) were used to identify groups within the samples. The data were further visualized via the PCA, Uniform Manifold Approximation and Projection (UMAP), and t-distributed Stochastic Neighbor Embedding (t-SNE) dimensional reduction techniques. Seurat's *FindAllMarkers* function identified genes specific to each cluster, with previous annotations indicating that genes were clustered by stages in cell differentiation. Feature plots for specific differentiation features were visualized in a t-SNE plot and through heatmaps for each cluster using Seurat's *DoHeatMap* and *FeaturePlot* functions. Pseudotime analysis was performed using the Slingshot package in R to visualize the cell differentiation process. To visualize the overlap in cell markers between human and mouse cells, the Euler package was used to generate a Venn diagram.

Data Records

Sequencing data have been submitted to the NCBI Gene Expression Omnibus (GSE226365)[22]. The dataset consists of raw sequencing data in FASTQ format, separated by the time point: D0 3T3-L1 and D0 SGBS (GSM7073976) and D5 3T3-L1 and D8 SGBS (GSM7073977). In addition, we provide processed data, separated by time point and cell line, including *barcodes.tsv*, *genes.tsv* and *matrix.mtx* files, listing raw UMI counts for each gene (feature) in each cell (barcode) in a sparse matrix format as supplementary files. R Data files for processed Seurat data objects, gene marker tables, and quality control summaries can be found in the GEO submission[22] and on the github repository.

Technical Validation

To validate the quality of our data, we investigated the technical quality and the unsupervised clustering and its reproducibility between the two datasets.

Quality control of the scRNA-Seq dataset. Interpretation of single-cell transcriptomics data is highly sensitive to technical artifacts. Sequencing data alignment using Cell Ranger led to the identification of comparable numbers of human and mouse cells within each of the analysed time points, as expected (Fig. 2a,b, Table 1). We used further steps to filter cells, removing any multiplets and cells with fewer than 200 genes detected (Fig. 2c,d, Table 2).

Annotation of cell subpopulations. Adipogenesis is a highly heterogeneous process, and we expected the addition of differentiation stimuli to result in the appearance of additional cell states compared to D0 of differentiation, prior to the exposure to differentiation media. In fact, for both 3T3-L1 and SGBS cells we identified three cell clusters whose transcriptional profiles suggest they are preadipocytes, differentiating cells and adipocytes, which is supported by the pseudotime analysis (Figs. 3a–c, 4a–c). Furthermore, in both cell models there was a clear separation of cells isolated at D0, which corresponded to the preadipocyte clusters, and cells isolated after the induction of adipogenesis (D5 in 3T3-L1, D8 in SGBS), which corresponded to the other clusters (Figs. 3d,e, 4d,e). Our scRNA-Seq dataset includes cells collected at two separate timepoints and processed independently, therefore we cannot rule out the presence of a batch effect contributing to the separation of D0 cells from later time points, which is a limitation of this study. However, analysis of the genes enriched in the identified cell clusters supports the view that the treatment with differentiation media affects the transcriptome, regardless of whether the cells fully differentiate, resulting in the differences between the clusters at D0 and D5/D8. In particular, adipogenesis is associated with major changes in the composition of the extracellular matrix (ECM) components. In line with previously published work, the preadipocyte cluster in SGBS cells showed enrichment in the expression of claudin 11 (*CLDN11*)[23], and the clusters containing differentiating cells both in SGBS and 3T3-L1 models showed an enrichment of the expression of collagen type III alpha 1 chain (*COL3A1*, *Col3a1*) which is associated with adipogenic differentiation[24]. Furter, adipocyte markers fatty acid binding protein 4 (*FABP4*)[25,26], adiponectin (*ADIPOQ*)[27], and perilipin 4 (*PLIN4*)[28] were identified in the SGBS adipocyte cluster and *Fabp4*[25,26], lipoprotein lipase (*Lpl*)[29], and resistin (*Retn*)[30] were identified in the 3T3-L1 adipocyte cluster (Figs. 3f, 4f, 5–7, Table 3). Full list of marker genes is provided as a.csv file with the GEO submission (#GSE226365)[22].

Code availability

All analytical code used for processing and technical validation is available on the GitHub Repository (https://github.com/christopherjin/SGBS_3T3-L1_differentiation_scRNASeq). The provided R code was run and tested using R 4.2.2.

References

1. Scheja, L. & Heeren, J. The endocrine function of adipose tissues in health and cardiometabolic disease. *Nat. Rev. Endocrinol.* **15**, 507–524 (2019).
2. Frayn, K., Karpe, F., Fielding, B., Macdonald, I. & Coppack, S. Integrative physiology of human adipose tissue. *Int. J. Obes. Relat. Metab. Disord.* **27**, 875–888 (2003).
3. Tang, W. *et al.* White fat progenitor cells reside in the adipose vasculature. *Science* **322**, 583–586 (2008).
4. Smith, U. & Kahn, B. B. Adipose tissue regulates insulin sensitivity: role of adipogenesis, de novo lipogenesis and novel lipids. *J. Intern. Med.* **280**, 465–475 (2016).
5. Mackall, J., Student, A., Polakis, S. E. & Lane, M. Induction of lipogenesis during differentiation in a" preadipocyte" cell line. *J. Biol. Chem.* **251**, 6462–6464 (1976).
6. Wabitsch, M. *et al.* Characterization of a human preadipocyte cell strain with high capacity for adipose differentiation. *Int. J. Obes. Relat. Metab. Disord.* **25**, 8–15 (2001).
7. Tews, D. *et al.* 20 Years with SGBS cells-a versatile *in vitro* model of human adipocyte biology. *Int. J. Obes. (Lond)* **46**, 1939–1947 (2022).
8. Kuri-Harcuch, W., Velez-delValle, C., Vazquez-Sandoval, A., Hernández-Mosqueira, C. & Fernandez-Sanchez, V. A cellular perspective of adipogenesis transcriptional regulation. *J. Cell Physiol.* **234**, 1111–1129 (2019).
9. Park, B. O., Ahrends, R. & Teruel, M. N. Consecutive positive feedback loops create a bistable switch that controls preadipocyte-to-adipocyte conversion. *Cell Rep.* **2**, 976–990 (2012).
10. Allott, E. H. *et al.* The SGBS cell strain as a model for the *in vitro* study of obesity and cancer. *Clin. Transl. Oncol.* **14**, 774–782 (2012).
11. Vijay, J. *et al.* Single-cell analysis of human adipose tissue identifies depot-and disease-specific cell types. *Nat. Metab.* **2**, 97–109 (2020).
12. Hildreth, A. D. *et al.* Single-cell sequencing of human white adipose tissue identifies new cell states in health and obesity. *Nat. Immunol.* **22**, 639–653 (2021).
13. Hepler, C. *et al.* Identification of functionally distinct fibro-inflammatory and adipogenic stromal subpopulations in visceral adipose tissue of adult mice. *Elife* **7**, e39636 (2018).
14. Schwalie, P. C. *et al.* A stromal cell population that inhibits adipogenesis in mammalian fat depots. *Nature* **559**, 103–108 (2018).
15. Emont, M. P. *et al.* A single-cell atlas of human and mouse white adipose tissue. *Nature* **603**, 926–933 (2022).
16. van Harmelen, V., Skurk, T. & Hauner, H. Primary culture and differentiation of human adipocyte precursor cells. *Human cell culture protocols*, 125–135 (2005).
17. Church, C., Berry, R. & Rodeheffer, M. S. Isolation and study of adipocyte precursors. *Methods in enzymology* **537**, 31–46 (2014).
18. Fink, T. & Zachar, V. Adipogenic differentiation of human mesenchymal stem cells. *Methods Mol. Biol.* **698**, 243–251 (2011).
19. Bengestrate, L. *et al.* Genome-wide profiling of microRNAs in adipose mesenchymal stem cell differentiation and mouse models of obesity. *PLoS One* **6**, e21305 (2011).
20. Godwin, L. A. *et al.* A microfluidic interface for the culture and sampling of adiponectin from primary adipocytes. *Analyst* **140**, 1019–1025 (2015).
21. Hao, Y. *et al.* Integrated analysis of multimodal single-cell data. *Cell* **184**, 3573–3587 (2021).
22. Li, J., Jin, L., Bielczyk-Maczynska, E. & Knowles, J. W. *GEO*. https://identifiers.org/geo/GSE226365 (2023).
23. Ullah, M., Sittinger, M. & Ringe, J. Extracellular matrix of adipogenically differentiated mesenchymal stem cells reveals a network of collagen filaments, mostly interwoven by hexagonal structural units. *Matrix Biol.* **32**, 452–465 (2013).
24. Al Hasan, M., Martin, P. E., Shu, X., Patterson, S. & Bartholomew, C. Type III collagen is required for adipogenesis and actin stress fibre formation in 3T3-L1 preadipocytes. *Biomolecules* **11**, 156 (2021).
25. Bernlohr, D. A., Angus, C. W., Lane, M. D., Bolanowski, M. A. & Kelly, T. Jr. Expression of specific mRNAs during adipose differentiation: identification of an mRNA encoding a homologue of myelin P2 protein. *PNAS* **81**, 5468–5472 (1984).
26. Matarese, V. & Bernlohr, D. Purification of murine adipocyte lipid-binding protein. Characterization as a fatty acid-and retinoic acid-binding protein. *J. Biol. Chem.* **263**, 14544–14551 (1988).
27. Hu, E., Liang, P. & Spiegelman, B. M. AdipoQ Is a Novel Adipose-specific Gene Dysregulated in Obesity. *J. Biol. Chem.* **271**, 10697–10703 (1996).

28. Wolins, N. E. *et al*. Adipocyte protein S3-12 coats nascent lipid droplets. *J. Biol. Chem.* **278**, 37713–37721 (2003).
29. Semenkovich, C., Wims, M., Noe, L., Etienne, J. & Chan, L. Insulin regulation of lipoprotein lipase activity in 3T3-L1 adipocytes is mediated at posttranscriptional and posttranslational levels. *J. Biol. Chem.* **264**, 9030–9038 (1989).
30. Steppan, C. M. *et al*. The hormone resistin links obesity to diabetes. *Nature* **409**, 307–312 (2001).
31. Chan, S. S., Schedlich, L. J., Twigg, S. M. & Baxter, R. C. Inhibition of adipocyte differentiation by insulin-like growth factor-binding protein-3. *Am. J. Physiol. Endocrinol. Metab.* **296**, E654–E663 (2009).
32. Quinkler, M., Bujalska, I. J., Tomlinson, J. W., Smith, D. M. & Stewart, P. M. Depot-specific prostaglandin synthesis in human adipose tissue: a novel possible mechanism of adipogenesis. *Gene* **380**, 137–143 (2006).
33. Ambele, M. A., Dessels, C., Durandt, C. & Pepper, M. S. Genome-wide analysis of gene expression during adipogenesis in human adipose-derived stromal cells reveals novel patterns of gene expression during adipocyte differentiation. *Stem Cell Res.* **16**, 725–734 (2016).
34. Song, N.-J. *et al*. Small molecule-induced complement factor D (Adipsin) promotes lipid accumulation and adipocyte differentiation. *PLoS One* **11**, e0162228 (2016).
35. Morales, L. D. *et al*. Further evidence supporting a potential role for ADH1B in obesity. *Sci. Rep.* **11**, 1932 (2021).
36. Christy, R. *et al*. Differentiation-induced gene expression in 3T3-L1 preadipocytes: CCAAT/enhancer binding protein interacts with and activates the promoters of two adipocyte-specific genes. *Genes Dev.* **3**, 1323–1335 (1989).
37. Yang, X. *et al*. The G0/G1 switch gene 2 regulates adipose lipolysis through association with adipose triglyceride lipase. *Cell Metab.* **11**, 194–205 (2010).
38. Anand, A. & Chada, K. *In vivo* modulation of Hmgic reduces obesity. *Nat. Genet.* **24**, 377–380 (2000).
39. Watanabe, T. *et al*. Annexin A3 as a negative regulator of adipocyte differentiation. *J. Biochem.* **152**, 355–363 (2012).
40. Hung, S.-C., Chang, C.-F., Ma, H.-L., Chen, T.-H. & Ho, L. L.-T. Gene expression profiles of early adipogenesis in human mesenchymal stem cells. *Gene* **340**, 141–150 (2004).
41. Li, C. *et al*. Matrix Gla protein regulates adipogenesis and is serum marker of visceral adiposity. *Adipocyte* **9**, 68–76 (2020).
42. Kansara, M. S., Mehra, A. K., Von Hagen, J., Kabotyansky, E. & Smith, P. J. Physiological concentrations of insulin and T3 stimulate 3T3-L1 adipocyte acyl-CoA synthetase gene transcription. *Am. J. Physiol.* **270**, E873–E881 (1996).

Acknowledgements

Author contributions

J.L. conceived the project, conducted experiments and analysed the data; C.J. conducted bioinformatic analyses, created figures and wrote the manuscript; S.G. assisted with bioinformatic analysis; A.R. assisted with bioinformatic analysis; M.W. provided critical resources for the project; C.Y.P. conceived the project and assisted with the experiments; T.Q. guided the bioinformatic analysis and critically reviewed the manuscript; E.B.M. analysed data, created figures and wrote the manuscript with the input from all the authors; J.W.K. oversaw the project and critically reviewed the manuscript.

Competing interests

The authors declare no competing interests.

Additional information

Correspondence and requests for materials should be addressed to J.W.K. or E.B.-M.

Reprints and permissions information is available at www.nature.com/reprints.

Publisher's note Springer Nature remains neutral with regard to jurisdictional claims in published maps and institutional affiliations.